Keldysh study of point-contact tunneling between superconductors

Bolech Gret, Carlos José; Giamarchi, Thierry

How to cite

BOLECH GRET, Carlos José, GIAMARCHI, Thierry. Keldysh study of point-contact tunneling between superconductors. In: Physical review. B, Condensed matter and materials physics, 2005, vol. 71, n° 2. doi: 10.1103/PhysRevB.71.024517

This publication URL: https://archive-ouverte.unige.ch/unige:36133
Publication DOI: 10.1103/PhysRevB.71.024517

Keldysh study of point-contact tunneling between superconductors

C. J. Bolech and T. Giamarchi
Université de Genève, DPMC, 24 Quai Ernest Ansermet, CH-1211 Genève 4, Switzerland
(Received 16 September 2004; published 25 January 2005)

We revisit the problem of point-contact tunnel junctions involving one-dimensional superconductors and present a simple scheme for computing the full current-voltage characteristics within the framework of the nonequilibrium Keldysh Green function formalism. We address the effects of different pairing symmetries combined with magnetic fields and finite temperatures at arbitrary bias voltages. We discuss extensively the importance of these results for present-day experiments. In particular, we propose ways of measuring the effects found when the two sides of the junction have dissimilar superconducting gaps and when the symmetry of the superconducting states is not the one of spin-singlet paring. This last point is of relevance for the study of the superconducting state of certain organic materials like the Bechgaard salts and, to some extent, for ruthenium compounds.

DOI: 10.1103/PhysRevB.71.024517 PACS number(s): 74.50.+r, 74.20.Rp, 74.70.Kn, 74.70.Pq

I. INTRODUCTION

The theory of superconductivity by Bardeen, Cooper, and Schrieffer (BCS) is one of the most important achievements of condensed matter theory. Some of the most striking consequences of this theory concern the tunneling to and from a superconductor. Indeed, the history of tunneling experiments and applications is strongly linked to that of superconductivity. Not only some of the most crucial experimental verifications of the BCS theory came from tunneling experiments,[1] but also some of the most important practical applications of superconductivity involve Josephson tunneling junctions. To describe the manifold of experimental and practical situations, two limiting cases are usually considered: planar interfaces and point contacts. As of latter, point-contact tunneling *per se* acquired renewed relevance with the development of scanning tunneling microscopy (STM),[2–4] that is today at the forefront of the experimental techniques used to study unconventional superconductors. For STM the tip can be modeled using some idealized geometry. For example the cases of spherical,[5,6] conical,[7,8] and pyramidal[9] tip geometries were considered in the literature (the last two were used to model very close STM contacts). The point-contact approximation is therefore the simplest one for the kind of tunneling processes that take place on STM experiments. Other ways to realize point contacts include the use of break junctions and pressed crossed wires.

The simplest theoretical models used to interpret experiments involving superconducting tunneling are typically based on a simple scattering picture and go generally under the name of *semiconducting band models*.[10–12] A more systematic approach is that based on the tunneling Hamiltonian.[13–15] A large series of recent experiments[16–21] on atomic-size contacts showed impressive agreement with the theory; achieving, some of them, detailed microscopic description of the contacts. The current transport in these systems can be described as taking place through a small number of independent *conduction channels*, each of them well described by a point-contact model. In some experiments even the observation of single-channel transport was possible.

Tunneling can thus be used as a very efficient probe of the properties of the leads. In particular one can expect to use it to determine the symmetry of the superconducting order parameter in the leads. However, the previous theoretical analyses of point-contact tunneling, although efficient in simple cases, are too cumbersome to be easily generalized to more complex cases such as unconventional order parameters at finite temperatures and finite magnetic fields. Simplified semiclassical methods exist,[22–24] but they suffer from their own limitations, for instance when one is dealing with anisotropic superconductors.[25] Thus a general and simple microscopic theory of point-contact tunneling was clearly lacking, and is necessary in order to take into account some of the complications of unusual superconductivity. Providing such a theory is the purpose of this work. We use a Keldysh formalism, to be able to compute the full current-voltage characteristics and gain access to the effects of external magnetic fields, potential scattering barriers, and finite temperatures on the transport properties of different junctions at arbitrary finite voltages. Contrarily to previous implementations of this technique, using the solution of difference equations,[15] we here obtain and diagonalize the full tunneling action for the point contact tunneling junctions involving normal-metal and superconductor leads. This allows one to easily incorporate complications such as triplet pairing in the leads, finite temperature, and finite magnetic field. We explore in particular the physical properties of tunneling systems with leads with triplet pairing parameters.

Indeed, although the possibility of having triplet pairing was investigated[26,27] soon after the BCS theory, and such an unconventional scenario was found about the same time in the *p*-wave spin-triplet superfluid state of ^{3}He,[28–30] the quest to identify a *p*-wave charged superfluid proved much more challenging. A class of candidates for triplet pairing, though the evidence is as yet not completely conclusive, are the organic superconductors[31,32] and the ruthenates.[33,34] There are also proposals of spin-triplet pairing phases for some heavy fermion superconductors like UPt_3, but the issue remains more open in those cases.[35] The organic compounds are the most interesting for us due to the quasi-one-dimensional nature of their normal phases, and also because

there is currently considerable debate on the symmetry of the superconducting phase.[36–38] For the ruthenates, on the other hand, the triplet pairing seems already backed up by a considerable amount of experimental evidence.[39,40] To sort out this question of the symmetry of the order parameter, tunneling can thus be an invaluable tool. Recently, STM tunneling experiments were used to study the symmetry of the superconducting phase of Sr_2RuO_4 and other compounds. No such attempts were as yet made in the case of the quasi-one-dimensional organic salts, but efforts in this direction are on their way. Also recently, preliminary experiments involving junctions between two (different) Bechgaard salts were performed, and they showed a number of puzzling features including a zero-bias conductance peak ("anomaly") and zero excess current.[41] In that context, a precise theory of the particularities of point-contact tunneling involving spin-triplet superconductors, done in the microscopic framework of the tunneling Hamiltonian models, was called for. Given the nature of these systems, it is difficult to perform phase sensitive experiments such as the ones that were, for the cuprates, smoking guns to fix the symmetry of the order parameter. We show, however, that the tunneling spectrum has characteristic features, such as the magnetic field dependence, that can be used to unambiguously determine the order parameter symmetry in these systems. A short account of part of the results of this paper was published previously.[42]

The rest of the paper is organized as follows. In Sec. II we present the model that we use to describe the point-contact junction geometry between either normal or superconducting leads. In Sec. III we work out a way of finding the tunneling characteristics using a nonequilibrium (Keldysh) formalism. This allows us to obtain the current-voltage characteristics for arbitrary current, temperature, or magnetic field, for junctions with either normal, or singlet or triplet superconducting leads. All technical details have been confined to these two sections, while the two remaining sections deal with the physical consequences of our findings. Readers only interested in those can thus safely jump to Sec. IV, where the physics of such junctions is discussed in detail. Those results are put in context within different experimental possibilities in Sec. V. In particular we discuss there the possibility of using tunneling experiments to probe the nature of the superconducting pairing in the organic superconductors. In Sec. VI we close the paper with a general discussion of the implications of our results.

II. MODEL OF THE POINT-CONTACT JUNCTION

Using a nonequilibrium Keldysh formalism we calculate the full current-voltage characteristics of different types of tunnel junctions where each side of the junction can be either a normal metal (N), a singlet (S), or a triplet (T) superconductor. We start from a tunneling Hamiltonian formulation,

$$H = H_1 + H_2 + H_{\rm tun}, \tag{1}$$

$$H_{\rm tun} = \sum_{\ell,\ell',\sigma} t_{\ell\ell'} \psi^\dagger_{\ell\sigma}(0)\psi_{\ell'\sigma}(0). \tag{2}$$

The first two terms describe the two leads of the junction (superconducting or otherwise) and the third one models the tunneling processes in which an electron with spin σ hops from lead ℓ' into lead ℓ. The tunneling matrix is

$$t_{\ell\ell'} = \begin{pmatrix} V_1 & t^* \\ t & V_2 \end{pmatrix}. \tag{3}$$

The diagonal terms, V_n, are local contact potential terms included for the sake of generality[43] and the off-diagonal ones are the tunneling matrix elements taken to be constant consistently with the assumption of a point contact. Since the number of particles in each lead is a conserved quantity in the absence of tunneling, we can define the current as proportional to the rate of change in the relative particle number and write[13]

$$I = \frac{e}{2}\langle \partial_t (N_2 - N_1)\rangle = \frac{e}{2i}\langle [H_{\rm tun}, N_1 - N_2]\rangle. \tag{4}$$

Notice that the diagonal part of the tunneling matrix conserves particle numbers and will not contribute to the current.

To model the superconducting leads in calculations intended to capture the main features of point-contact transport on conventional superconductors, very simple models suffice to achieve even quantitative agreement with the experiment. Contrary to the case in some planar junction experiments, dimensionality plays little or no role in the tunneling. Therefore one can use one-dimensional leads to carry out all the standard calculations. The situation becomes more complex in the case of unconventional superconductors, mainly because the anisotropic nature of the pair wave function has to be taken into account when modeling the leads. The most conspicuous case is that of the cuprate compounds, for which the putative *d*-wave pairing cannot be modeled within a single-band one-dimensional lead. On the other hand, the organic superconductors that we are interested in are supposed to have *p*-wave symmetry. Since both *s*-wave and *p*-wave symmetries can be modeled in single-band one-dimensional chains, we can conveniently set up a formalism that encompasses the two cases, as well as the normal state. In the following, we will consider a one-dimensional band with two Fermi points and expand the fermion fields around them in the conventional way,[44]

$$\psi_\sigma(x) \approx e^{-ik_F x}\psi_{L\sigma}(x) + e^{ik_F x}\psi_{R\sigma}(x) \tag{5}$$

thus defining left and right moving fields (lead indexes were omitted here). Using these fields and in the spirit of the BCS theory, we introduce the following four gap functions:

$$\Delta_a(x) = \lambda_a \langle \alpha \psi_{L\bar{\alpha}}(x)\sigma^a_{\alpha\beta}\psi_{R\beta}(x)\rangle \tag{6}$$

where Greek indexes are summed over, $a=0,\ldots,3$ and $\sigma^0_{\alpha\beta}$ is the identity matrix while the other three are the usual Pauli matrices. We use the notation $\bar{\alpha}=-\alpha$ with $\alpha \in (\downarrow,\uparrow) \equiv (-1,+1)$.[68] The constants λ_a would depend on the details of the microscopic pairing mechanism about which we make no assumptions.[36] With this definition $\Delta_0(x)$ is the spin-singlet order parameter, as in conventional superconductors, and the other three functions form a vector of spin-triplet order parameters,[39] $\vec{\Delta}(x)=\Delta(x)\hat{d}(x)$. We use the approximation of dropping the spatial dependence in the order parameter and,

directly in Fourier space, we write the Hamiltonian for any of the two leads as

$$K = \xi_{ck\sigma}\psi^{\dagger}_{ck\sigma}\psi_{ck\sigma} - \{\Delta_a[\psi^{\dagger}_{Rk\beta}\sigma^a_{\beta\alpha}\alpha\psi^{\dagger}_{Lk\bar{\alpha}}] + \text{H.c.}\}$$

where $K=H-\mu N$ with μ the chemical potential of that lead. All the indexes are summed over, in particular $c \in (L,R) \equiv (-1,+1)$ sums over the two possible chiralities and $\xi_{ck\sigma} = cv_F k - \mu - \sigma h$ are the corresponding linear dispersions, shifted by the inclusion of chemical potential and magnetic field along the $\hat{z}$ axis (for convenience we will take $v_F=1$). This is the natural extension to the triplet case of the usual pairing-approximation Hamiltonian found in BCS theory, we remark that the fact it does not conserve particle number is an artifact of the anomalous mean field approximation behind its derivation and has no bearing in the operator definition of the current.

III. LOCAL ACTION APPROACH

Within the extended-BCS framework, the Hamiltonian remains a quadratic form including "anomalous" terms. To be able to write it down as a canonical quadratic form we introduce the following spinor notation:

$$\Psi_{kn\sigma}(\varpi) = \begin{pmatrix} \psi_{Rk\sigma}(\varpi) \\ \sigma\psi^{\dagger}_{Lk\bar{\sigma}}(\bar{\varpi}) \end{pmatrix} \equiv \begin{pmatrix} \psi_{Rk\uparrow}(\varpi) \\ \psi_{Rk\downarrow}(\varpi) \\ \psi^{\dagger}_{Lk\downarrow}(\bar{\varpi}) \\ -\psi^{\dagger}_{Lk\uparrow}(\bar{\varpi}) \end{pmatrix} \tag{7}$$

(that we present directly in Fourier space). Here k is the reduced momentum (after linearization was carried out) and

$$\varpi = \omega - \mu \tag{8}$$

is the shifted frequency corresponding to a time evolution given by K (cf. with the discussion of tunneling given in Ref. 45); here the bars have the meaning of minus signs. Since we make explicit distinction between chiralities, all the components of the spinor are independent. Using this basis the Hamiltonian can be written in matrix form

$$K_{sc} = \Psi^{\dagger}_{kn\sigma}(\varpi)\begin{bmatrix} \xi_{k\sigma}\hat{\sigma}^0_{\sigma\tau} & -\hat{\Delta}_{\sigma\tau} \\ -\hat{\Delta}^{\dagger}_{\sigma\tau} & -\xi_{k\bar{\sigma}}\hat{\sigma}^0_{\sigma\tau} \end{bmatrix}_{nm} \Psi_{km\tau}(\varpi). \tag{9}$$

Here we arranged the different components of the order parameter using the following matrix notation:

$$\hat{\Delta} = \begin{pmatrix} \Delta_{\downarrow\uparrow} & \Delta_{\uparrow\uparrow} \\ \Delta_{\downarrow\downarrow} & \Delta_{\uparrow\downarrow} \end{pmatrix} \equiv \Delta_a\hat{\sigma}^a = \begin{pmatrix} \Delta_0+\Delta_3 & \Delta_1 - i\Delta_2 \\ \Delta_1 + i\Delta_2 & \Delta_0 - \Delta_3 \end{pmatrix}.$$

We note that another convention, the one introduced in the work of Balian and Werthamer,[26] is related to ours via $\hat{\Delta}_{BW} = \hat{\Delta}\cdot(i\hat{\sigma}^y)$; the difference is rooted in a different definition of the spinor basis.

In the case of zero magnetic field, K^2 is block diagonal and one arrives to a closed solution for the quasiparticle excitation spectrum.[28] In the presence of magnetic field the calculations for the case of a general order parameter are more involved. We adopt the convention of taking the quantization axis ($\hat{z}$) along the magnetic field direction and consider the cases of triplet order parameters parallel or perpendicular to the field. In both of these cases the Hamiltonian can be diagonalized via a canonical rotation (i.e., a Bogoliubov-Valatin transformation) that proceeds in a completely identical way to that of the conventional s-wave case. Following the analogy further, the local Green functions for the leads can be written down immediately. For the case of a parallel order parameter (i.e., $\Delta_1=\Delta_2=0$) the nonzero matrix elements of the advanced and retarded Green functions are

$$g^{r,a}_{11} = g^{r,a}_{33} = \frac{2}{w}\frac{-(\varpi + h \pm i\eta)}{\sqrt{|\Delta_{\downarrow\uparrow}|^2 - (\varpi + h \pm i\eta)^2}}, \tag{10}$$

$$g^{r,a}_{13} = [g^{r,a}_{31}] = \frac{2}{w}\frac{\Delta^{[*]}_{\downarrow\uparrow}}{\sqrt{|\Delta_{\downarrow\uparrow}|^2 - (\varpi + h \pm i\eta)^2}}, \tag{11}$$

$$g^{r,a}_{22} = g^{r,a}_{44} = \frac{2}{w}\frac{-(\varpi - h \pm i\eta)}{\sqrt{|\Delta_{\uparrow\downarrow}|^2 - (\varpi - h \pm i\eta)^2}}, \tag{12}$$

$$g^{r,a}_{24} = [g^{r,a}_{42}] = \frac{2}{w}\frac{\Delta^{[*]}_{\uparrow\downarrow}}{\sqrt{|\Delta_{\uparrow\downarrow}|^2 - (\varpi - h \pm i\eta)^2}}, \tag{13}$$

with the upper (lower) sign corresponding to the retarded (advanced) ones. Here $w=4v_F$ is an energy scale related to the Fermi velocity (or equivalently to the normal density of states at the Fermi level) and η is a positive infinitesimal that regularizes the Green functions (sometimes kept finite to model the inelastic relaxation processes inside the leads). Analogously for the case of a perpendicular order parameter (i.e., $\Delta_0=\Delta_3=0$), the nonzero matrix elements of the advanced and retarded Green functions are this time

$$g^{r,a}_{11} = g^{r,a}_{44} = \frac{2}{w}\frac{-(\varpi \pm i\eta)}{\sqrt{|\Delta_{\uparrow\uparrow}|^2 - (\varpi \pm i\eta)^2}}, \tag{14}$$

$$g^{r,a}_{14} = [g^{r,a}_{41}] = \frac{2}{w}\frac{\Delta^{[*]}_{\uparrow\uparrow}}{\sqrt{|\Delta_{\uparrow\uparrow}|^2 - (\varpi \pm i\eta)^2}}, \tag{15}$$

$$g^{r,a}_{22} = g^{r,a}_{33} = \frac{2}{w}\frac{-(\varpi \pm i\eta)}{\sqrt{|\Delta_{\downarrow\downarrow}|^2 - (\varpi \pm i\eta)^2}}, \tag{16}$$

$$g^{r,a}_{23} = [g^{r,a}_{32}] = \frac{2}{w}\frac{\Delta^{[*]}_{\downarrow\downarrow}}{\sqrt{|\Delta_{\downarrow\downarrow}|^2 - (\varpi \pm i\eta)^2}}. \tag{17}$$

The nonequilibrium formalism that we seek to implement in order to access the full I-V characteristics for arbitrary finite voltages, requires the introduction of one more linearly independent Green function. From the expressions for the retarded and advanced functions and using the assumption of thermal equilibrium of the leads, we can construct immediately the so-called Keldysh component[46] of the local lead Green function: $g^k_{ij} = (g^r_{ij} - g^a_{ij})\tanh(\varpi/2T)$.

Before proceeding, we stop to comment on the case of two normal leads. The corresponding Green functions are obtained by using any of the two sets above and taking the

limit $\Delta_a \to 0 \,\forall\, a$. In this case it is a simple exercise to derive from Eq. (4) the well-known expression for the conductance of an N-N junction:

$$G_{NN} = \frac{e^2}{\pi\hbar}\alpha \quad \text{with } \alpha = \frac{4t^2}{(1+t^2)^2}, \tag{18}$$

where we reintroduced Plank's constant and measured t in units of w. This expression was first derived by Landauer and later extended and generalized in the works of Büttiker, Imry, and others.[47] The constant α is called the *channel transparency* and takes values in the interval [0,1]. Now we return to the case when at least one of the two leads is superconducting.

Given the local Green functions and the tunneling Hamiltonian, the simplest way to proceed in order to compute the characteristics of a junction is to use linear response and perturbation theory.[14,45] A more rigorous approach should make use of nonequilibrium Green functions and treat the tunneling term to all orders. This, to be able to calculate the full I-V line and give a quantitative account of its subgap structure even in the ballistic limit (i.e., for $\alpha \to 1$). One past implementation of this program made a clever use of the nonequilibrium Dyson equations and reduced the problem to the solution of a set of linear recursion relations.[15] Here we do not want to restrict ourselves to the *s*-wave case and to zero temperature and fields, we shall take then a different route. We treat the local action and Green functions directly as matrices in order to gain the convenience of a simpler implementation of multiband multicomponent spinors and deal with them numerically.

We notice that the lead Green functions can be inverted in close analytical form to obtain the corresponding local lead actions. This procedure implies the assumption of fast relaxation rates,[1] which is consistent with the point-contact geometry of the junction. Namely, working in a Keldysh-extended Nambu-Eliashberg spinor basis of symmetric and antisymmetric combinations of forward and backward time paths (see Ref. 46), the local action for a single lead can be written as

$$S_\ell = \int \frac{d\omega}{2\pi} \Psi^\dagger_{\kappa n,\ell} [\mathcal{A}_\ell]_{\kappa n,\kappa' n'} \Psi_{\kappa' n',\ell}, \tag{19}$$

where n labels the different components of the four-spinors as introduced in Eq. (7) and κ is the index for the two (symmetric and antisymmetric) Keldysh components. The matrix representation of the spinorial action density is given by

$$\mathcal{A}_\ell \equiv \begin{pmatrix} \hat{0} & \hat{g}^a \\ \hat{g}^r & \hat{g}^k \end{pmatrix}^{-1} = \begin{pmatrix} -[\hat{g}^r]^{-1}\hat{g}^k[\hat{g}^a]^{-1} & [\hat{g}^r]^{-1} \\ [\hat{g}^a]^{-1} & \hat{0} \end{pmatrix}, \tag{20}$$

where $\hat{g}^{r,a,k}$ are the matrices in the four-spinor basis whose nonzero components were given above (for the two orientations of the order parameter that we will consider, the inverses of $\hat{g}^{r,a}$ are easy to calculate in closed form). By combining these actions and the spinorial matrix representation of the tunneling Hamiltonian ($\mathcal{H}_{\text{tun}}$) written in a two-lead Keldysh-extended Nambu-Eliashberg spinor basis, one can ensemble the full nonequilibrium action matrix density for the junction

$$\mathcal{A} = [\mathcal{A}_{\ell=1} \oplus A_{\ell=2}] - H_{\text{tun}}. \tag{21}$$

While carrying out this construction, special attention must be paid to the fact that the shifted frequencies [see Eq. (8)] will have different reference levels when there is a relative bias applied to the leads. Positively and negatively shifted frequencies in each lead are related by the coherent pairing processes in the superconductors; this is reflected on the choice of frequency pairs in the spinor basis. When two superconductors with different chemical potentials are put into contact, the tunneling Hamiltonian connects real (i.e., *unshifted*) frequencies. Thus, at finite voltages, pairing and tunneling together create an infinite set of related frequencies that is at the heart of the multiparticle tunneling processes mediated by the so-called Andreev reflections; this is illustrated in Fig. 1.

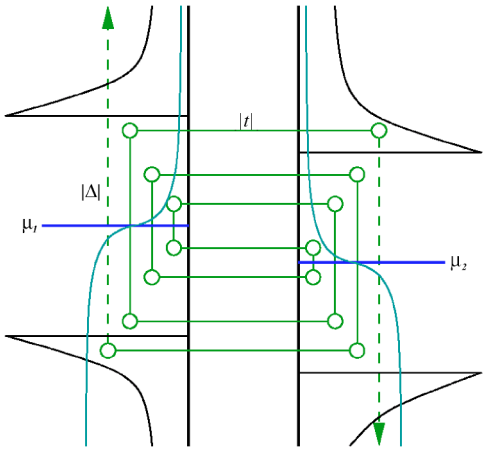

FIG. 1. Depiction of a set of frequencies involved in a multiple coherent tunneling process (the vertical axis corresponds to frequencies). The horizontal lines correspond to frequency-conserving tunneling processes that take place with amplitude $|t|$, while the vertical lines correspond to electron (hole) pair creation or destruction processes that occur with amplitude $|\Delta|$ (the superconducting gap is taken in this figure to have the same magnitude in the two sides of the junction). The chemical potentials, thermal distributions, and superconducting quasiparticle densities of states in the leads are schematically indicated. The lowest order nonzero contribution to the tunneling is depicted. The dashed lines and arrows indicate that the chain of interrelated higher order processes continues *ad infinitum*.

To each value in the frequency window defined by the chemical potentials in the two leads, one such set of "entangled" frequencies can be assigned. These sets are independent and the action is block diagonal between different ones. Discretizing the frequencies in this window automatically defines a discretization of the "whole" frequency space. We proceed in this way and deal with one such set of frequencies at a time. Since these sets are infinite, we truncate their hierarchies at some distance from the central frequency window. This is equivalent to introducing a *soft* limit in the number of allowed Andreev reflections: up to some fixed number (N_A) they are fully taken into account and then they

are gradually suppressed until twice that number is reached. This is a natural and consistent cutoff scheme at any finite voltage, since the presence of a growing frequency denominator makes the higher contributions less and less important regardless of the value of α. It is also clear what the limitations of the approach are; as the difference in chemical potentials decreases, the denominators grow more and more slowly and a larger number of Andreev reflections is required in order to achieve the same accuracy.

The implementation of the described scheme imports one more complication. In the spinor basis we adopted, only chirality conserving tunneling processes can be written in matrix form. To overcome this problem we introduce a second *mirrored* spinor basis with the chiralities inverted [as in Eq. (7) but interchanging $R \leftrightarrow L$]. Using two copies of the spinor space the full tunneling Hamiltonian (that is, including chirality nonconserving processes) can be written as a matrix and the *whole* frequency space for *both* chiral species is considered (let us stress that no Hilbert space doubling takes place). Inverting the action matrix density thus constructed [Eq. (21)], using standard numerical methods, we can obtain frequency densities for the different current harmonics (constructed out of the Keldysh components of lead-mixing Green functions). Here we will concentrate on the dc component. Finally, the current is computed integrating its density over the full frequency axis,

$$I = \frac{et}{2i}\sum_{\sigma} \int \frac{d\omega}{2\pi} \langle \psi^{\dagger}_{2,\sigma}\psi_{1,\sigma} - \psi^{\dagger}_{1,\sigma}\psi_{2,\sigma}\rangle_{\mathrm{kel}}. \qquad (22)$$

The practical implementation of this numerical scheme is straightforward and allows one to consider the (combined) effects of finite temperature, applied magnetic fields, contact potentials in the junction, spin-flip tunneling, or spin-flip scattering processes[48] in the leads. It is also possible to compute the ac response. Here our primary interest is in comparing singlet and triplet superconductor junctions and how they respond differently in the presence of an external field or with temperature; other additional complications will be discussed elsewhere. Even though our numerical scheme is not well suited for studying the limit $V \to 0$, in particular the combination $\alpha \sim 1$ with $V \sim 0$ is the computationally most expensive one, that limit can nevertheless be approached analytically. On the other hand, all other regimes can be solved with modest computational effort and the algorithm is quite easily parallelizable. Even more, we shall show that the finite bias features are the ones that might provide useful signatures to further establish the spin-triple scenario.

IV. TUNNELING CHARACTERISTICS

To discuss and compare the I-V characteristics for different types of junctions, we choose some convenient set of parameters that clearly display the different features. For the tunneling overlap integral we choose the values $t=0.2$ and $t=0.5$ (that correspond, in the notation of Ref. 11, to $\alpha \simeq 0.15$ or $Z=2.4$ and to $\alpha=0.64$ or $Z=0.75$, respectively), and when there is a magnetic field we fix its value to $h=0.2$ in units of Δ (by Δ we mean the magnitude of the singlet gap, Δ_0, or of the triplet vector order parameter depending on the case; notice we absorbed Bohr's magneton and the gyromagnetic factor in the definition of the magnetic field). These values are larger than, for instance, those in the most typical STM tunneling experiments, except for the ones engineered expressly to seek for large values of α,[17] but have the virtue of making evident the different features, including the Andreev gap structure (see below). We show, except when indicated, curves for the dc response in the limit of vanishing temperatures. For the truncation procedure we have taken $N_A=3$ and $N_A=5$ for the cases of $t=0.2$ and $t=0.5$, respectively (and verified that larger values produce, given the set of parameters chosen, identical curves). The discretization used on the horizontal axis is better than $\delta V = 0.025\Delta/e$ in all the cases.

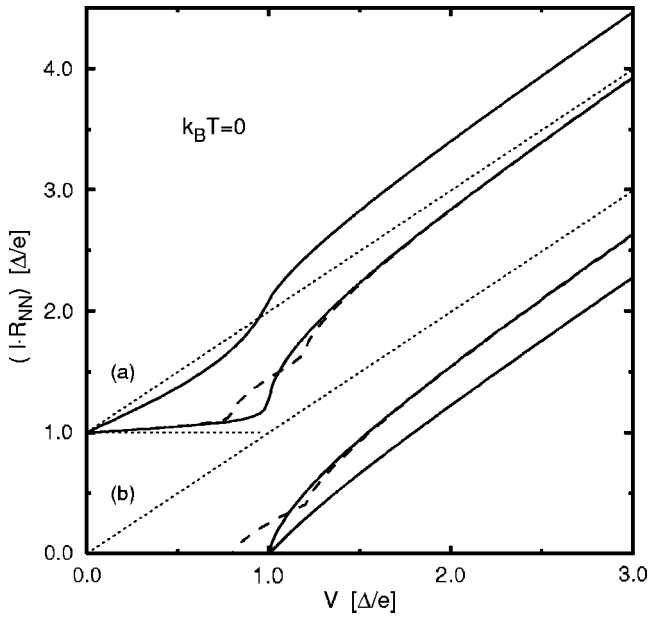

FIG. 2. Zero temperature I-V characteristics of normal-superconductor junctions for both spin-singlet and spin-triplet paring. (a) N-S junctions for $t=0.2$ (lower curves) with and without applied magnetic field (dashed and solid lines, respectively, $h=0.2$) and $t=0.5$ (upper curve, solid line only since the effect of field is smaller and not displayed); the curves are vertically displaced for clarity. (b) N-T junctions for $t=0.2$ (upper curve) with and without applied magnetic field (dashed and solid lines, respectively, $h=0.2$) and $t=0.5$ (lower curve, solid line only).

We review now the different pairing-symmetry scenarios. Let us start with the case of normal-metal–superconductor junctions. We show in Fig. 2(a) typical curves for an N-S junction (i.e., a point-contact junction between a normal metal and a conventional singlet-pairing superconductor). The diagonal straight line is the N-N characteristics given as a reference. The solid lines correspond to the N-S junction in zero field and the dashed line is for one of the junctions (the less transparent one) in the presence of a magnetic field. The effect of the magnetic field is to produce what would be seen as a Zeeman splitting of the differential conductance peak (i.e., the peak in the curve of dI/dV vs V). Notice the subgap shoulder on the I-V curve when $eV<\Delta$ (for instance in the zero field case); its origin is in the coherent Andreev pro-

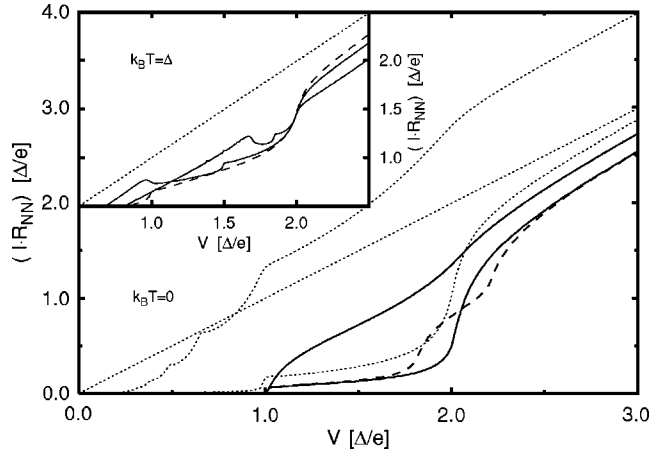

FIG. 3. Zero temperature I-V characteristics of S-T junctions with and without magnetic field (dashed and solid lines, respectively, $h=0.2$). The lower solid and dashed curves are for $t=0.2$ (without and with magnetic field) and the upper solid curve is for $t=0.5$. The dotted lines are (i) the straight unitary slope line for the reference N-N characteristics and (ii) the S-S characteristics for similar-parameters junctions (upper $t=0.5$ and lower $t=0.2$). The inset shows finite temperature characteristics of S-S junctions with different values of the left and right gap amplitudes. The dotted line is the reference N-N characteristics and the dashed line is the curve for $\Delta_2=\Delta_1$. The solid lines correspond to $\Delta_2\neq\Delta_1$ ($\Delta_2=3\ \Delta_1$ for the line closest to the dashed one and $\Delta_2=37/3\ \Delta_1$ for the other one).

cesses that take place at the junction contact. Next we show in Fig. 2(b) a typical curve this time for what we call an N-T junction (i.e., a junction between a normal metal and an unconventional triplet-pairing superconductor). The solid lines correspond to the N-T junction in zero field and the dashed line is for the $t=0.2$ junction when in the presence of a magnetic field that is aligned with the vector order parameter $\vec{\Delta}$. If one considers a magnetic field that is perpendicular to the order parameter ($\vec{h}\perp\vec{\Delta}$), one finds it has no effect on the I-V characteristic that remains identical to the one for the zero field case (remark that in the case of the N-S junction the orientation of the field was immaterial). Notice also the absence of a subgap shoulder on the I-V curve. This absence is caused by the odd real-space symmetry of the superconductor (*p*-wave pairing): Andreev processes with opposite chiralities interfere destructively and exactly cancel each other. As a result, the curves are exactly identical to those computed with a semiconducting band model that ignores Andreev scattering (to be contrasted with the nontrivial results in this respect that will be shown momentarily for junctions involving two different-symmetry superconductors).

Let us now turn to examine the case of junctions in which both their sides are superconducting. In Fig. 3 we display typical curves for S-S junctions (both the sides are conventional spin-singlet superconductors) and S-T junctions (one of the sides is a spin-triplet superconductor). The straight dotted line is the N-N characteristics—taken as a reference, same as before. The remaining dotted lines are the I-V curves of S-S junctions that show all the standard features already well documented in the literature.[12,15] For the purpose of later comparison, we remark here the sizeable currents for voltages $eV>2\Delta$ (the value of the gap is taken to be the same on both sides of the junction), and the "subgap" shoulder with Andreev steps at $eV=2\Delta/n$ (with $n=1,2,3,\ldots$). We also remind the reader that this curve is, when orbital effects can be ignored, not sensitive to applied magnetic fields. The remaining curves (dashed and solid lines) correspond to S-T junctions with different tunneling matrix element strengths and with and without magnetic field (respectively). The solid lines are insensitive to the orientation of the vector order parameter on the triple-pairing side of the junctions, and the current amplitude is found to be systematically smaller than in the case of the respective S-S junctions. Remarkably, the "subgap" structure shows only two steps (at voltages given by $n=1,2$) and the current is zero when $eV<\Delta$ (if the magnitudes of the gaps in the spin-singlet and spin-triplet sides of the junction are different, then the zero current condition is $eV<\Delta_{\mathrm{Triplet}}$, where $\Delta_{\mathrm{Triplet}}$ is the magnitude of the vector order parameter on the spin-triplet side of the junction). Concerning the effects of an applied magnetic field, the curves remain unchanged if the field is applied parallel to the direction of the vector-order parameter, but show instead a Zeeman effect if the field is perpendicular to it (dashed line). This is in contrast with the case of N-T junctions, for which the Zeeman effect is expected for fields $\vec{h}\|\vec{\Delta}$.

In the figure inset we display curves for S-S junctions at finite temperatures. In order to render the different features simultaneously visible, we "push" the temperature to be equal to Δ (with $k_B=1$). Let us denote as Δ the average gap value ($2\Delta=\Delta_1+\Delta_2$) that we keep using to define the unit in which we measure the voltage, normalized current, etc. The dashed line is the finite temperature I-V for the $t=0.2$ junction between two identical superconductors ($\Delta_2=\Delta_1$), whereas the solid lines correspond to similar junctions with $\Delta_2=3\ \Delta_1$ or $\Delta_2=37/3\ \Delta_1$ and the same transparency (during this discussion we assume $\Delta_2\geqslant\Delta_1$). Besides the standard quasiparticle tunneling threshold ($eV=2\Delta$) one clearly sees in both solid curves the step at $eV=\Delta_2$ corresponding to the first term of the so-called *even series* ($eV=2\Delta_\ell/m$ with $\ell=1,2$ and $m=2,4,\ldots$). The steps corresponding to the *odd series* ($eV=2\Delta/m$ with $m=3,5,\ldots$) are not visible in this plot, but we verified that we observe them at low temperatures in junctions with $\Delta_2\gtrsim\Delta_1$. This current step structure lacks temperature or magnetic field dependence (in accordance with experimental observations). The other prominent feature of the solid curves is the rounded cusp at $eV\approx\Delta_2-\Delta_1$. This is a thermally activated feature that appears when the upper gap edges at both sides of the junctions are aligned. The rounding of the cusp has similar origin as the rounding of the quasiparticle threshold, both are due to higher order multiparticle processes. One new observation that we made is that the position of the thermal cusp is not exactly $\Delta_2-\Delta_1$, but it is shifted towards lower voltages. This is again a result of taking into account higher order Andreev processes and is made more evident by our choice of parameters; for lower temperatures and less transparent junctions this correction is typically very small. We also find that the steps of both the even and the odd series that fall to the left of the thermal cusp are usually washed away by its tail; this

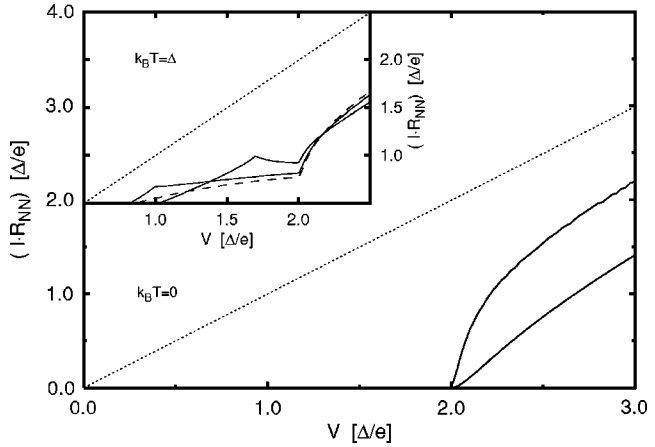

FIG. 4. Zero temperature I-V characteristics of T-T junctions. The lower curve corresponds to $t=0.5$ and the upper one to $t=0.2$. The dotted line is the reference N-N characteristics. The inset shows finite temperature characteristics of T-T junctions with different values of the left and right gap amplitudes. We used the same value choices as in the inset of Fig. 3. Namely, the dotted line is the N-N characteristics and the dashed line corresponds to $\Delta_2=\Delta_1$ while the solid lines are for $\Delta_2\neq\Delta_1$ ($\Delta_2=3\ \Delta_1$ for the line closest to the dashed one and $\Delta_2=37/3\ \Delta_1$ for the other one).

we find to be consistent with available experimental results. We expect the different detailed features corresponding to dissimilar gaps and finite temperatures to be accessible to current state-of-the-art experiments, we will comment on that in the next section.

As an aside, let us comment on the effect of local contact potential terms in the tunneling matrix. They suppress uniformly the dc current amplitude but have no other effect on the shape of the I-V characteristics. This is true regardless of the pairing symmetry of the superconductors forming the junction, in particular they do not cause the appearance of midgap states in the case of triplet pairing (for neither the N-T or S-T junctions nor for the T-T junctions discussed below).

Finally, the only remaining case to consider is that of junctions in which both sides are spin-triplet superconductors. Such a case is exemplified in the curves of Fig. 4. Andreev processes with triplet symmetric pairing, for tunneling through a single-mode contact, interfere destructively and the current remains zero up to voltages larger than $eV=2\Delta$, when quasiparticle tunneling becomes allowed. The lower solid line corresponds to $t=0.5$ and the upper one to $t=0.2$, the inversion of the order is due to the fact that, for this range of parameters, the current at fixed voltage grows more slowly than in the case of normal junctions (N-N). Similarly as in the S-S case, both sides of the junction react identically to applied magnetic fields and no net effects are therefore visible in the current-voltage characteristics.

The curves in the figure inset are the same as in the inset of the previous figure but for the case of spin-triple pairing symmetry (on both sides of the junction). Both the quasiparticle tunneling threshold and the thermal cusp remain sharp since higher order processes interfere destructively and no rounding takes place. Another consequence of this is that the position of the thermal cusp is exactly $eV=\Delta_2-\Delta_1$ and no shift is observed. The subgap part of the curves is smooth and its height and shape are governed by the thermal excitations, the step structure of the even and odd series is absent. Also in this case magnetic fields have no direct effects.

V. EXPERIMENTAL CONSEQUENCES

A first set of applications concerns atomic contacts. For the case of normal or singlet superconducting leads with identical gaps, and zero temperature and magnetic field, our results are in full agreement with the previous studies of such systems.[15] For the case of two different gaps shown in the inset of Fig. 3, our theory correctly reproduces the different steps as discussed in the previous section. Another prominent feature of such curves is the thermally activated rounded cusp at $eV\approx\Delta_2-\Delta_1$. The rounding is due to higher order multiparticle processes; and a new prediction is that the position of the thermal cusp is not exactly $\Delta_2-\Delta_1$, but it is shifted towards lower voltages. Such a shift from the naive "density of states" answer could in principle be checked directly in atomic contacts. We also find that the steps of both the even and the odd series that fall to the left of the thermal cusp are usually washed away by its tail; this we find to be consistent with available experimental results.[1] Such features corresponding to dissimilar gaps and finite temperatures should be accessible to current state-of-the-art experiments. For instance, the experiments of Ref. 17 could be attempted using a Pb STM tip as before but to prove into a Mn-doped Pb sample. Mn will act as a magnetic impurity and decrease the value of the gap, such a setup would correspond to the situation of similar but not identical gap parameters with a doping controllable difference; it would be a way to try to observe the "splitting" of the even series in single-point contacts. Other setups could be envisaged based also on STM techniques or on pressed crossed wires.

The main application of our results, however, concerns the use of tunneling with triplet superconductors.[42] In that case the most direct experimental realization is organic superconductors.[32] The experiments show that for magnetic fields along the direction of the conducting chains (**a** crystalline axis) the upper critical field is paramagnetically limited. If such systems are indeed triplet superconductors, this would correspond, following our notations, to a vector order parameter aligned with the field ($\vec{h}\|\vec{\Delta}$).[49] With this geometry a Zeeman splitting of the differential conductance peak, similar to that in conventional superconductors, should be observed in a tunneling experiment. As the field is rotated the splitting would be suppressed and for a magnetic field oriented parallel to the $\mathbf{b}'$ crystalline axis there should be no Zeeman effect (accompanied by the possibility of applying large fields that are not paramagnetically limited). The disappearance of splitting even as the field is being increased would constitute a clear signature of spin-triplet superconductivity. The main difficulties of such an experiment would be the set up of point-contacts and the resolution required to observe the Zeeman effect. On the first point one possibility would be to use STM setups with "thin tips." On the second

point, since the critical temperature of these organic salts is relatively low, the experiment could be done with moderate fields that would produce splittings that are a substantial fraction of the superconducting gap. The linearity of the magnetic field dependence of these splittings, a signature of the Zeeman effect, could be accurately established using Fourier analysis techniques.[50]

Similarly as in the case of N-T junctions, we can envisage using the Zeeman response of S-T junctions as a direct probe for spin-triplet order. If, for instance, a magnetic field is applied along the $\mathbf{b}'$ crystalline axis of $(TMTSF)_2PF_6$, we predict a Zeeman splitting of the main differential conductance peak. This would also constitute a clear sign of unconventional superconductivity since such an effect does not take place for standard BCS superconductors. The $\mathbf{b}'$ direction is the one on which the upper critical field is not paramagnetically limited, so relatively large fields could be applied in order to obtain a clear signal (as the field alignment changes the splitting disappears). To afford large fields one would need to use in the "conventional" side of the junction a compound with a relatively high critical temperature [as compared with that of $(TMTSF)_2PF_6$]. In this respect one has the bonus that, since the required setup should be a point-contact, superconductivity might survive at the contact-neck region up to fields much in excess of the bulk value of H_{c2} (rather approaching H_p^{BCS} for that material).[8,51] Another advantage in the two-superconductor setup is that the levels of noise are usually smaller,[52] allowing a better definition of the differential conductance signal from where the Zeeman splitting is going to be read off.

Similar considerations could also be made for those layered compounds that are believed to be triplet superconductors.[31,53] In that case the critical magnetic field is not paramagnetically limited when the applied field is oriented parallel to the superconducting planes. Among these compounds Sr_2RuO_4 is the best studied one so far, but only few tunneling experiments were performed,[54–58] and none so far with high resolution and in the presence of an applied external magnetic field (see though Refs. 56, 57, and 59). One of the conspicuous features observed in some of these experiments is the presence of a "zero bias anomaly" (ZBA) in the differential conductance. Its explanation is still a matter of debate, but seems to require extended contact interfaces and momentum dependent order parameters (to include the effect of "zero energy states" at the interfaces, extensions to our scheme would be required, possibly incorporating certain aspects of those calculations already done for planar junctions[60–62]). Our general findings about the effect of magnetic fields should, however, apply, since they refer to effects to be measured at voltages of the order of the superconducting gap. It is intriguing to notice that in the "point-contact" experiment of Ref. 55 two types of spectra are measured: with and without ZBA in the differential resistance. One might speculate that what changes between the different samples should be no other thing than the effective size, potential barrier, and geometry of the contact (experiments in other compounds indicate that that might be enough to give rise to zero voltage features; cf. Ref. 63). In particular, if that is the case, at least those dV/dI curves with no ZBA should, according to our calculations, show no Zeeman splitting when a field is applied parallel to the Ru-O planes, in contrast to what is expected for BCS superconductors. Two different groups reported that further point contact and STM tunneling experiments on Sr_2RuO_4 in a magnetic field are underway.[55,64]

VI. SUMMARY AND CLOSING REMARKS

Summarizing, we have shown how the full I-V characteristics for point-contact junctions can be accurately studied using a local action approach in the context of the Keldysh formalism. Our formalism allows one to treat both normal and superconducting (singlet and triplet) leads, and to take into account effects of finite magnetic field and temperature. In particular we have shown that the point-contact tunneling involving unconventional superconductors with spin-triplet pairing displays interesting characteristic features. Unlike the case of conventional superconductors, these show quite different characteristics whether the junctions are planar[65] or point-contact-like.[42] The Zeeman response to an external magnetic field is such that it allows for the identification of triplet phases and might be relevant for future experiments. The prediction of a truncated subgap structure in point-contact S-T junctions is also very interesting, but experiments to test this are much harder to carry out. These kinds of detailed experiments are, however, possible for conventional superconductors and we believe they could be exploited to look for some as yet poorly tested predictions of the theory. For instance, the experiments of Ref. 17 could be attempted using a Pb STM tip as before but doping the sample with Mn; it would be a way to try to observe the "splitting" of the even series in single-point contacts.

Besides the different additional effects on the tunneling characteristic that we discussed here (the effects of fields, temperature, and contact potentials), there are others that can also be easily taken into account like, for instance, spin-flip tunneling processes or temperature gradients. These effects will be relevant in the study of junctions involving ferromagnets (of possible relevance in the context of spintronics; cf. Ref. 66) or in precision studies related to the renewed interest in the use of microjunctions for *on-chip* thermometry and eventually cryogenics.[67] A remaining challenge, however, is how to extend our formalism seeking to include the physics responsible for producing ZBAs in order to further our understanding of tunneling experiments in layered unconventional superconductors and planar junctions. Such extensions shall seek to describe not only the point-contact limit, but also the planar interface case. This is one of the ingredients necessary for a realistic description of layered materials like the ruthenates. In that respect the interplay with the advances already made using semiclassical methods will constitute not only a check of the approximations made in the latter but also a way of finding efficient computational schemes for more complicated scenarios that might incorporate, for instance, the two-band nature of certain compounds. On the other hand, in the context of the quasi-one-dimensional organic conductors, such developments should help to go beyond the one-dimensional approximation.

ACKNOWLEDGMENTS

We would like to thank Ø. Fischer, M. Eskildsen, M. Kugler, and G. Levy for discussions about tunneling and STM. We also thank Y. Maeno and M. Sigrist for discussions about tunneling into triplet superconductors and ruthenates in particular. This work was done under the auspices of the Swiss National Science Foundation and its MaNEP program.

[1] E. L. Wolf, *Principles of Electron Tunneling Spectroscopy*, Vol. 71 of *International Series of Monographs on Physics*, 2nd ed. (Oxford University Press, Clarendon Press, Oxford, 1989).
[2] C. F. Quate, Phys. Today **39**, 26 (1986).
[3] G. Binnig and H. Rohrer, Rev. Mod. Phys. **59**, 615 (1987).
[4] G. Binnig and H. Rohrer, Rev. Mod. Phys. **71**, S324 (1999).
[5] J. Tersoff and D. R. Hamann, Phys. Rev. Lett. **50**, 1998 (1983).
[6] J. Tersoff and D. R. Hamann, Phys. Rev. B **31**, 805 (1985).
[7] H. Suderow, E. Bascones, W. Belzig, F. Guinea, and S. Vieira, Europhys. Lett. **50**, 749 (2000).
[8] H. Suderow, E. Bascones, A. Izquierdo, F. Guinea, and S. Vieira, Phys. Rev. B **65**, 100519(R) (2002).
[9] J. C. Cuevas, A. L. Yeyati, and A. Martín-Rodero, Phys. Rev. Lett. **80**, 1066 (1998).
[10] J. Nicol, S. Shapiro, and P. H. Smith, Phys. Rev. Lett. **5**, 461 (1960).
[11] G. E. Blonder, M. Tinkham, and T. M. Klapwijk, Phys. Rev. B **25**, 4515 (1982).
[12] M. Octavio, M. Tinkham, G. E. Blonder, and T. M. Klapwijk, Phys. Rev. B **27**, 6739 (1983).
[13] M. H. Cohen, L. M. Falicov, and J. C. Phillips, Phys. Rev. Lett. **8**, 316 (1962).
[14] J. W. Wilkins, *Tunneling Phenomena in Solids*, 1st ed. (Plenum Press, New York, 1969), Chap. 24, p. 333.
[15] J. C. Cuevas, A. Martín-Rodero, and A. L. Yeyati, Phys. Rev. B **54**, 7366 (1996).
[16] E. Scheer, P. Joyez, D. Esteve, C. Urbina, and M. H. Devoret, Phys. Rev. Lett. **78**, 3535 (1997).
[17] E. Scheer, N. Agraït, J. C. Cuevas, A. L. Yeyati, B. Ludoph, A. Martín-Rodero, G. Rubio-Bollinger, J. M. van Ruitenbeek, and C. Urbina, Nature (London) **394**, 154 (1998).
[18] B. Ludoph, N. van der Post, E. N. Bratus', E. V. Bezuglyi, V. S. Shumeiko, G. Wendin, and J. M. van Ruitenbeek, Phys. Rev. B **61**, 8561 (2000).
[19] E. Scheer, W. Belzig, Y. Naveh, M. H. Devoret, D. Esteve, and C. Urbina, Phys. Rev. Lett. **86**, 284 (2001).
[20] G. Rubio-Bollinger, C. de las Heras, E. Bascones, N. Agraït, F. Guinea, and S. Vieira, Phys. Rev. B **67**, 121407(R) (2003).
[21] M. Häfner, P. Konrad, F. Pauly, J. C. Cuevas, and E. Scheer, Phys. Rev. B **70**, 241404(R) (2004).
[22] J. C. Cuevas and M. Fogelström, Phys. Rev. B **64**, 104502 (2001).
[23] J. Kopu, M. Eschrig, J. C. Cuevas, and M. Fogelström, Phys. Rev. B **69**, 094501 (2004).
[24] A. Millis, D. Rainer, and J. A. Sauls, Phys. Rev. B **38**, 4504 (1988).
[25] N. Kopnin, *Theory of Nonequilibrium Superconductivity*, Vol. 110 of *International Series of Monographs on Physics*, 1st ed. (Oxford Science Publications, Clarendon Press, Oxford, 2001).
[26] R. Balian and N. R. Werthamer, Phys. Rev. **131**, 1553 (1963).
[27] P. W. Anderson and P. Morel, Phys. Rev. **123**, 1911 (1961).
[28] P. W. Anderson and W. F. Brinkman, *Proceedings of the 15 Scottish Universities Summer School in Physics*, edited by J. G. M. Armitage and I. E. Farquhar (Academic Press, New York, 1975), pp. 314–416.
[29] D. D. Osheroff, R. C. Richardson, and D. M. Lee, Phys. Rev. Lett. **28**, 885 (1972).
[30] D. D. Osheroff, W. J. Gully, R. C. Richardson, and D. M. Lee, Phys. Rev. Lett. **29**, 920 (1972).
[31] T. Ishiguro, in *High Magnetic Fields: Applications in Condensed Matter Physics and Spectroscopy*, Vol. 595 of *Lecture Notes in Physics*, edited by C. Berthier, L. P. Lévy, and G. Martinez (Springer-Verlag, Heidelberg, 2002), pp. 301–313.
[32] Chem. Rev. (Washington, D.C.) **104** (2004), special issue on Molecular Conductors.
[33] T. M. Rice and M. Sigrist, J. Phys.: Condens. Matter **7**, L643 (1995).
[34] G. Baskaran, *Proceedings of the International Conference on Strongly Correlated Electron Systems* [Physica B**224**, 490 (1996)].
[35] R. Joynt and L. Taillefer, Rev. Mod. Phys. **74**, 235 (2002).
[36] *ISCOM 2003—The Fifth International Symposium on Crystalline Organic Metals, Superconductors and Ferromagnets, Port-Bourgenay, September 21–26, 2003* [J. Phys. IV **114** (2004)].
[37] J. I. Oh and M. J. Naughton, Phys. Rev. Lett. **92**, 067001 (2004).
[38] N. Joo, P. Auban-Senzier, C. R. Pasquier, P. Monod, D. Jrome, and K. Bechgaard, Eur. Phys. J. B **40**, 43 (2004).
[39] A. P. Mackenzie and Y. Maeno, Rev. Mod. Phys. **75**, 657 (2003).
[40] T. M. Rice and M. Sigrist, Phys. Today **54**, 42 (2001).
[41] H. I. Ha, J. I. Oh, J. Moser, and M. J. Naughton, Synth. Met. **137**, 1215 (2003).
[42] C. J. Bolech and T. Giamarchi, Phys. Rev. Lett. **92**, 127001 (2004).
[43] I. Affleck, J. S. Caux, and A. M. Zagoskin, Phys. Rev. B **62**, 1433 (2000).
[44] T. Giamarchi, *Quantum Physics in One Dimension*, Vol. 121 of *International Series of Monographs on Physics*, 1st ed. (Oxford Science Publications, Clarendon Press, Oxford, 2004).
[45] G. D. Mahan, *Many-Particle Physics, Physics of Solids and Liquids* (Kluwer Academic/Plenum, New York, 2000), 3rd ed.
[46] L. V. Keldysh, Sov. Phys. JETP **20**, 1018 (1965).
[47] Y. Imry and R. Landauer, Rev. Mod. Phys. **71**, S306 (1999).
[48] C. Grimaldi and P. Fulde, Phys. Rev. B **56**, 2751 (1997).
[49] A. G. Lebed, K. Machida, and M. Ozaki, Phys. Rev. B **62**, R795 (2000).
[50] G. B. Hertel and T. P. Orlando, Phys. Rev. B **32**, 166 (1985).
[51] A. M. Clogston, Phys. Rev. Lett. **9**, 266 (1962).
[52] M. Eskildsen (private communication).
[53] V. Mineev, in *High Magnetic Fields: Applications in Condensed Matter Physics and Spectroscopy*, Vol. 595 of *Lecture Notes in Physics*, edited by C. Berthier, L. P. Lévy, and G. Martinez (Springer-Verlag, Heidelberg, 2002), pp. 287–300.

[54] R. Jin, Y. Liu, Z. Q. Mao, and Y. Maeno, Europhys. Lett. **51**, 341 (2000).
[55] F. Laube, G. Goll, H. v. Löhneysen, M. Fogelström, and F. Lichtenberg, Phys. Rev. Lett. **84**, 1595 (2000).
[56] Z. Q. Mao, K. D. Nelson, R. Jin, Y. Liu, and Y. Maeno, Phys. Rev. Lett. **87**, 037003 (2001).
[57] M. D. Upward, L. P. Kouwenhoven, A. F. Morpurgo, N. Kikugawa, Z. Q. Mao, and Y. Maeno, Phys. Rev. B **65**, 220512(R) (2002).
[58] M. Kugler (private communication).
[59] A. Sumiyama, T. Endo, Y. Oda, Y. Yoshida, A. Mukai, A. Ono, and Y. Ōnuki, Physica C **367**, 129 (2002).
[60] M. Yamashiro, Y. Tanaka, and S. Kashiwaya, Phys. Rev. B **56**, 7847 (1997).
[61] C. Honerkamp and M. Sigrist, J. Low Temp. Phys. **111**, 895 (1998).
[62] Y. Asano, Y. Tanaka, M. Sigrist, and S. Kashiwaya, Phys. Rev. B **67**, 184505 (2003).
[63] G. Sheet, S. Mukhopadhyay, and P. Raychaudhuri, Phys. Rev. B **69**, 134507 (2004).
[64] H. Kambara, K. Yokota, T. Matsui, I. Ueda, T. Shishido, M. Wada, N. Kikugawa, Y. Maeno, and H. Fukuyama, *Proceedings of the 23rd International Conference on Low Temperature Physics (LT23), Hiroshima, Japan, 20–27 August 2002* [Physica C **388–389**, 503 (2003)].
[65] K. Sengupta, I. Žutić, H.-J. Kwon, V. M. Yakovenko, and S. Das Sarma, Phys. Rev. B **63**, 144531 (2001).
[66] R. Lopez and D. Sanchez, Phys. Rev. Lett. **90**, 116602 (2003).
[67] J. Pekola, R. Schoelkopf, and J. Ullom, Phys. Today **57**, 41 (2004).
[68] Notice that the object $\alpha\psi_{L\bar{\alpha}}$ transforms as the complex conjugate representation of the fundamental representation of SU(2). In other words, it has the same transformation properties as $\psi^{\dagger}_{L\alpha}$.